CJC Chinese Journal of Chemistry
中国化学 - An International Journal

Accepted Article

Title: Fluorescence Sensing of Glutathione Thiyl Radical by BODIPY-Modified β-Cyclodextrin

Authors: Zhixue Liu, Xianyin Dai, Qiaoyan Xu, Xiaohan Sun, and Yu Liu*

This manuscript has been accepted and appears as an Accepted Article online.

This work may now be cited as: *Chin. J. Chem.* **2021**, *40,* 10.1002/cjoc.202100662.

The final Version of Record (VoR) of it with formal page numbers will soon be published online in Early View: http://dx.doi.org/10.1002/cjoc.202100662.

Liu Yu (Orcid ID: 0000-0001-8723-1896)

Cite this paper: *Chin. J. Chem.* **2021**, *39*, XXX—XXX. **DOI: 10.1002/cjoc.202100XXX**

Fluorescence Sensing of Glutathione Thiyl Radical by BODIPY-Modified β-Cyclodextrin

Zhixue Liu, Xianyin Dai, Qiaoyan Xu, Xiaohan Sun, and Yu Liu*

College of Chemistry, State Key Laboratory of Elemento-Organic Chemistry, Nankai University, Tianjin 300071, P. R. China

Keywords

Cyclodextrin | Glutathione thiyl radical | Fluorescence sensing | BODIPY | Radical cross-coupling reaction

Main observation and conclusion

The fluorescence sensing of intracellular glutathione thiyl radical (GS•) is in great demand to seek the GS•-related pathophysiological events. Herein, **BODIPY**-modified β-cyclodextrin was developed for high-efficiency sensing of GS•, accompanied by a fast response time ($t_{1/2}$ =218 s), with the limits of detection for 468 nM. Cell experiments indicated that the **BODIPY**-modified β-cyclodextrin could be applied to detect the GS• in live A549 cells.

Comprehensive Graphic Content

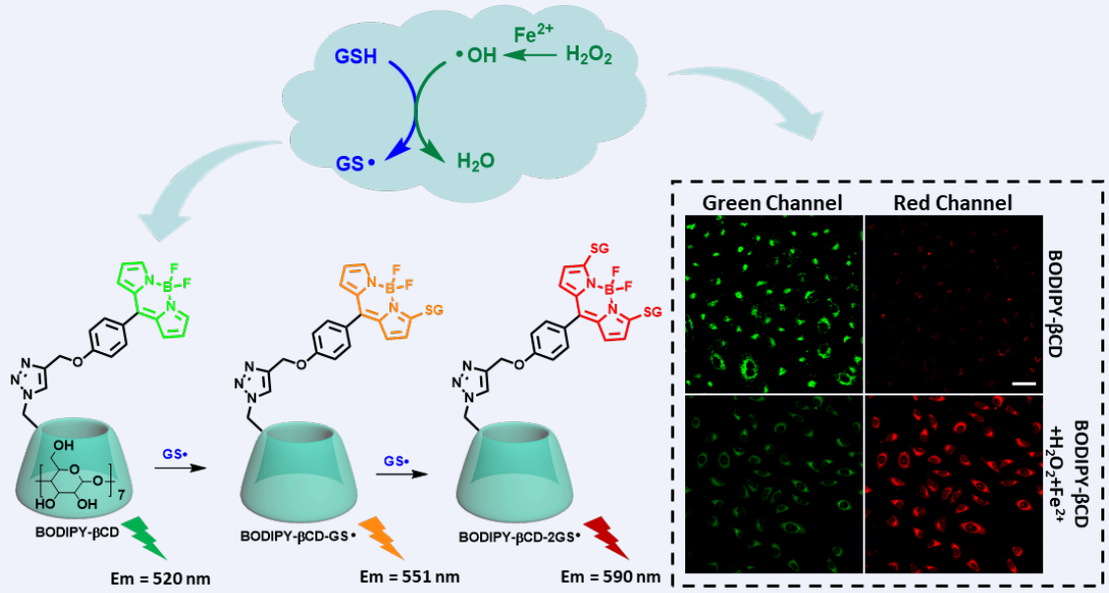

*E-mail: yuliu@nankai.edu.cn

View HTML Article | Supporting Information

Background and Originality Content

Thiyl radicals are important intermediates in thiol redox biology and chemistry, which involve a series of biological processes, including the mechanism of action of ribonucleotide reductase.[1-3] Among them, glutathione thiyl radical (GS•) is the direct product of the reaction between glutathione (GSH) and free radicals.[4] In the process of converting GSH to GS•, it can effectively scavenge free radicals produced in the process of human metabolism.[5-7] Meanwhile, the produced GS• can also function as an electron "sink" by removing radicals from α-carbon (C_α) position in the protein via hydrogen-atom transfer (HAT), thereby "repairing" the related protein radical damage.[8] On the other hand, GS• is a strong oxidant, which can cause cell damage by reacting with protein thiols and the unsaturated acyl chains of phospholipids.[9,10] Therefore, GS• plays a significant role in the intracellular redox process. Since the GSH is the highest concentration of non-protein biothiols,[11,12] and the GS• can be generated under oxidative stress or in the activation of signaling pathways, the accurate detection of GS• is in great demand to seek the GS•-related pathophysiological events.

Structurally, GS• has high chemical reactivity, short lifetime and poor stability, as well as easy to generate GSSG,[8,13,14] causing its analysis in biological systems to be blocked. The commonly used detection method is based on electron paramagnetic resonance spectroscopy spintrapping,[15] which undoubtedly makes the detection process very complicated. At present, fluorescent probes are widely used in the detection of GSH because of their high sensitivity, strong specificity, fast responses etc.[16-23] However, among the reported fluorescent probes, most types of them mainly depend on the nucleophilic properties of sulfhydryl groups to qualitative or quantitative detect GSH,[24-29] which cannot achieve effective sensing of GS•, resulting in the limitation of the in-depth understanding of GS• in cellular environments. Taking the above factors into account, introducing the organic reaction based on thiol radicals as the detection mechanism is expected to achieve rapid identification of GS•.

To our knowledge, thiol radicals have the characteristics of high activity and strong bonding ability, which have become one of the common strategies for C-S bond coupling reactions.[30-33] In 2019, Xie and coworkers reported an efficient and selective photocatalysis approach for introducing ArS units into **BODIPY** through thiyl radicals in THF.[34] The quantum yields of ArS-substituted **BODIPY** has been greatly improved. In the same year, Hao and Jiao *et al.* reported an efficient transition-metal-free regioselective C-H/S-H cross-coupling of **BODIPY** with thiols for controllable synthesis of mono-, di- and tri-thiolation **BODIPY** via a radical process in DMSO.[35] In addition, they also use the same mechanism to achieve α-sulfonylated **BODIPY**s with sodium sulfinates through oxidative radical hydrogen substitution in CH_3NO_2.[36] It was found that thiol radicals and **BODIPY** can effectively undergo radical cross-coupling reaction, which gave significant changes in fluorescence properties. However, these kinds of coupling reactions were mainly carried out in organic solvents, accompanied by the high temperature or the long reaction time. As far as we know, **BODIPY** has been extensively studied and used in the design of fluorescent probes for sensing of GSH,[37-40] that is to say, how to achieve and increase the rate of the thiol radicals cross-coupling reaction based on **BODIPY** derivatives in the aqueous phase is the key to achieve accurate detection of GS• in living cells.

One possible strategy to accomplish these tasks is to take advantage of supramolecular macrocyclic compounds, such as cyclodextrin (CD). CD is a "cone-shaped" molecule that own hydrophobic cavity and hydrophilic outer wall, which is composed of 6-8 α-D-glucopyranose units linked by α-1, 4-glycosidic bonds.[41-43] Up to now, the research of molecular recognition and molecular assembly based on CD have become a hot research field in supramolecular chemistry.[44-49] Among them, it is one of the commonly used strategies in the catalytic coupling reaction of the aqueous phase, such as Suzuki cross-coupling reaction.[50] The main reason is that the cavity of CD can interact with hydrophobic organic molecules to form a reversible host-guest inclusion complex, which improves the solubility of guest molecules in water and then enables organic reactions to proceed in water.[51] Meanwhile, under appropriate conditions, CD and its derivatives can play a selective catalytic role, and the hydroxyl group on the cone can also ensure that the reaction proceeds in a desired direction through hydrogen bonding.[52,53] Therefore, it is reasonable to modify the **BODIPY** with CD to achieve and increase the efficiency of free radical cross-coupling reaction in water.

In this study, we constructed a ratiometric fluorescent probe for highly selective sensing of intracellular GS• based on **BODIPY**-modified β-cyclodextrin (**BODIPY-βCD**) (Scheme 1). It exhibited a high affinity for GS• based on thiol radicals cross-coupling reaction, with the limits of detection for 468 nM. As the concentration of GS• increased, the fluorescence intensity changed obviously, and then reached the balance until the final concentration was 130 μM. Time-course fluorescence response spectra displayed the whole reaction process can be finished within 10 min, representing the completion of the radical cross-coupling reaction, accompanied by the observed rate constant (K_{obs}=3.18x10^{-3} s^{-1}) and a fast response time ($t_{1/2}$ = 218 s). Importantly, the covalent bonding connection between β-CD and the **BODIPY** was necessary, which not only improved the water solubility and biocompatibility, but also avoided the self-aggregation of **BODIPY**. In addition, the affinity of **BODIPY-βCD** for GS• was higher than **BODIPY**, making it useful for highly selective sensing of GS• in living cells. Through the cell experiments, it was found that the **BODIPY-βCD** had extremely low cytotoxicity and could be applied to detect the GS• in live A549 cells.

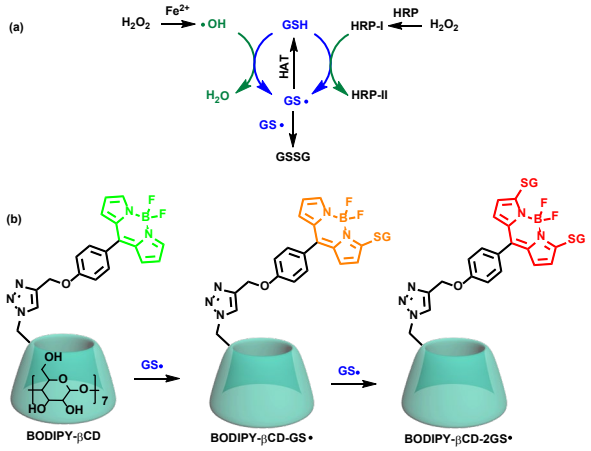

Scheme 1 (a) The generation and reaction of GS•. (HAT: Hydrogen-atom transfer; HRP: Horseradish peroxidase). (b) Molecular structure of **BODIPY-βCD** and the radical cross-coupling reaction with GS•.

Results and Discussion

It is well kown that Fe^{2+} could react with H_2O_2 to generate the hydroxyl radicals (•OH) based on the Fenton reaction,[54,55] and the •OH could react with GSH to generate the same equivalent of GS•. Therefore, in order to simulate the transformation of GSH to GS•, H_2O_2 was selected for the formation of •OH with Fe^{2+}. We first used UV–Vis absorption and fluorescence spectroscopy to evaluate the detection performance of **BODIPY-βCD** toward GS•. The solution of **BODIPY-βCD** was pre-treated with GSH (1 mM), and no obvious fluorescence changes were found even after 40 min (Figure S1). However, upon addition of the mixture of Fe^{2+} and H_2O_2, the absorption peak at 501 nm of **BODIPY-βCD** decreased rapidly, accompanied by two new peaks emerged at 536 nm and 575 nm

(Figure 1a), which occurred along with an obvious color change from pale yellow to purple (Figure 1a, inset). In this process, the absorption peak at 536 nm first increased and then declined when the peak at 575 nm reached the balance (Figure 1a and S2a). From the fluorescence spectroscopy of titration experiment, the emission peak of the **BODIPY-βCD** at 520 nm was decreased and two new peaks were gradually increased at 551 nm and 590 nm, accompanied by a distinct fluorescence color change from green to orange red (Figure 1b and 1c, inset). The emission peak at 551 nm first increased and then declined along with the further increment of peak at 590 nm, its trend was similar with UV−Vis absorption spectroscopy (Figure S2b and S2c). Meanwhile, superior ratiometric fluorescence responses were observed, accompanied by a large separation (ca. 74 nm). In the dose–response plots for the reaction between **BODIPY-βCD** and the GS•, we found the most obvious fluorescence change were around 0–130 μM, indicating that **BODIPY-βCD** could be used to detect GS• with highly affinity and sensitivity (Figure 1d). The limits of detection for GS• was calculated to be 468 nM based on an S/N ratio of 3 (Figure S3).

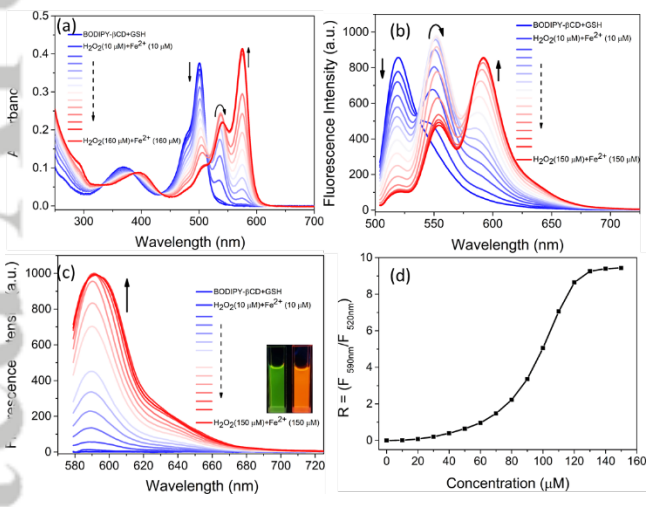

Figure 1 Changes in the UV-Vis absorption (a) and fluorescence spectra (b, c) of **BODIPY-βCD** (10 μM) pre-treated with GSH (1 mM) upon addition of Fe^{2+} and H_2O_2. [(b): Ex = 491 nm; (c): Ex = 565 nm]. (d) Dose–response curves of reactions of **BODIPY-βCD** toward GS• (GSH = 1 mM, Fe^{2+} = H_2O_2 = 0-150 μM).

In order to real-time monitor the process of the reaction, the time-course fluorescence response spectra were performed. It was found that the radical cross-coupling reaction between **BODIPY-βCD** and GS• can be finished within 10 min (Figure 2a). Obviously, the fluorescence emission at 551 nm was first increased and then declined, which was similar with the UV–Vis and fluorescence spectra. From the time-course fluorescence response spectra, we can obtain the observed rate constant (K_{obs}=3.18x10^{-3} s^{-1}) and a fast response time ($t_{1/2}$ = 218 s) (Figure S4). In addition, we selected UV–Vis and fluorescence spectra to assess the stability of **BODIPY-βCD** and the selectivity toward GS•. As showed in Figure S5, no obvious fluorescence changes were found for **BODIPY-βCD** in the condition of pH variations, while, it displayed excellent responsivity to GS• at pH 4–10. Furthermore, good selectivity for GS• was also achieved, with an enhancement of the fluorescence ratio (F_{590nm}/F_{520nm}) at least 2200-fold relative to that of various other intracellular amino acids, reactive oxygen (ROS) and nitrogen species (RNS) (Figure 2b and S6), suggesting that **BODIPY-βCD** was suitable for qualitative detection of GS• in living cells. In addition, due to the existence of large amount of H_2O_2 in cancer cells, we pre-treated with GSH (1 mM) and H_2O_2 (0.4 mM) in the solution of **BODIPY-βCD**, and then upon addition of the different concentration of Fe^{2+} (Figure S7). The UV–Vis and fluorescence spectra showed the similar results, and the obvious fluorescence changes were around 0–13 μM, demonstrating that the **BODIPY-βCD** could be used to monitor the variation of GS• depends on the concentration of Fe^{2+} in cancer cells.

Next, we explored the mechanism of the radical coupling reaction between **BODIPY-βCD** and GS•. From the UV–Vis spectroscopy, it was found that the emission peak of **BODIPY-βCD** did not gave obvious change in the presence of GSH, H_2O_2, Fe^{2+}, GSH+H_2O_2 or GSH+Fe^{2+} after 40 min (Figure S8). This comparison represents that the reaction only occurred in the presence of GSH+H_2O_2+Fe^{2+}, demonstrating that **BODIPY-βCD** could only react with the GS• rather than GSH. During the process of sensing, two new peaks indicated the formation of two products. Form the UV–Vis and fluorescence spectra, we can confirm that the one was the mono-substituted product for **BODIPY-βCD**+GS•, accompanied by 37 nm redshift,[25,56-58] another was the double-substituted product for **BODIPY-βCD**+2GS•, accompanied by 74 nm redshift.[34,59,60] These changes in UV–Vis and fluorescence spectra were consistent with the reported researches. Furthermore, MALDI-TOF studies were conducted to confirm the existence of double-substituted product. A mass peak at 2092.1981 corresponding to [**BODIPY-βCD**+2GS•+1] and the mass peak at 2147.0351 corresponding to [**BODIPY-βCD**+2GS•+Fe^{2+}] (Figure S9). On the other hand, we tested the influence of Fe^{3+} for the detection. It was well known that the Fe^{3+} could react with H_2O_2 to generate •OOH instead of •OH. Upon addition of Fe^{3+}, the similar fluorescent changes for **BODIPY-βCD** was observed, which confirmed that GSH could also react with •OOH to obtain GS• and can be used to detect the GS• depends on the concentration of Fe^{3+} (Figure S10). This result demonstrated that the **BODIPY-βCD** could be used to monitor the GS• after GSH reacted with various free radicals. In addition, it was well known that HRP could react with H_2O_2, and then generate the GS• in the presence of GSH, which have been confirmed by ESR (electron spin resonance) spectrum.[14] Therefore, we pre-treated with H_2O_2 and GSH in the solution of **BODIPY-βCD**, and then upon addition of the HRP. The UV–Vis spectra showed that the absorption peak at 501 nm of **BODIPY-βCD** decreased, and the two new peaks at 536 nm and 575 nm increased (Figure S11). This result confirmed that the GS• was gernated under the condition of HRP and H_2O_2, and then reached balance within 3 minutes. By using this fluorescent probe **BODIPY-βCD**, we can fast capture the production of GS• under oxidative stress, which will be helpful to seek the GS•-related pathophysiological events.

To demonstrate the advantages of β-CD in the sensing of GS•, we comparative analyzed the detection performance of **BODIPY** (Figure 2c). The molar absorptivity of **BODIPY** at 530 nm was very high, but not for **BODIPY-βCD**. The main reason may come from the aggregation of **BODIPY** due to its poor water solubility. After reacted with GS•, the molar absorptivity of **BODIPY** at 566 nm was much lower than **BODIPY-βCD**+2GS•. These results demonstrated that the **BODIPY-βCD** not only improved the water solubility of **BODIPY**, but also avoided the interference caused by self-aggregation of **BODIPY**. The related changes in the UV-Vis absorption of **BODIPY** toward GS• were displayed in Figure S12. Through the dose–response plots for the reactions between **BODIPY** and the GS•, we found the most obvious fluorescence changes were around 0–250 μM, indicating that **BODIPY** could also react with GS•, but the affinity was lower than **BODIPY-βCD**. In addition, to evaluate the effect of the covalent bond between the **BODIPY** and β-CD in **BODIPY-βCD**, we prepared nonbonded complex between β-CD and **BODIPY**, and evaluated its reaction with the GS• (Figure S13). Under these conditions, no obvious spectral changes were observed upon addition of the GS• in the absence or presence of β-CD, which demonstrated that simply mixing the **BODIPY** with β-CD did not improved the reaction efficiency, and also cannot avoid the self-aggregation of **BODIPY**, indicating that the covalent bonding connection between β-CD and the **BODIPY** was necessary.

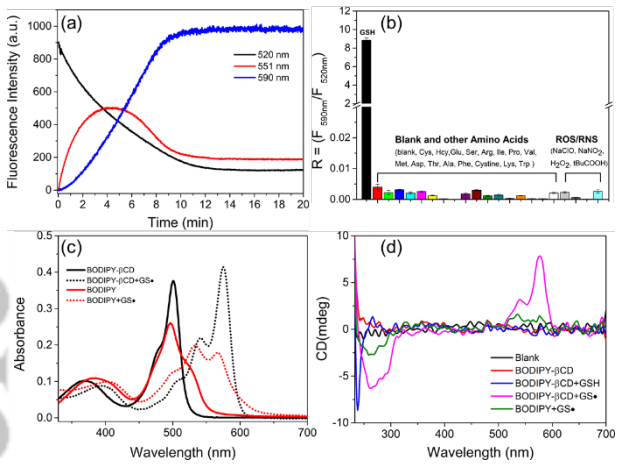

Figure 2 (a) Time-dependent fluorescence emission for **BODIPY-βCD** (10 μM) upon reaction with GS• (black: Ex = 491 nm; red: Ex = 526 nm; blue: Ex = 565 nm). (b) Ratiometric fluorescence response of **BODIPY-βCD** toward intracellular amino acids, ROS and RNS (0.1 mM). (c) Comparative analysis of **BODIPY-βCD** and **BODIPY** towards GS• in the UV-Vis absorption. (d) Circular dichroism spectra of **BODIPY-βCD** (10 μM) and **BODIPY** (10 μM) toward GS• in water. (GSH = 1 mM, Fe^{2+} = H_2O_2 = 120 μM).

After that, we measured the circular dichroism spectra to verify the spatial configuration of **BODIPY-βCD** (Figure 2d). The spectra of **BODIPY-βCD** displayed no Cotton effects, suggesting that the **BODIPY** unit was not encapsulated in the hydrophobic cavity of the β-CD. In addition, the linker between BODIPY and β-CD is rigid triazole and is too short to encapsulate BODIPY units in a self-inclusion mode. Hence, we deduced that the self-inclusion between BODIPY unit and β-CD was difficult at low concentration (10 μM). However, the **BODIPY-βCD**-2GS• showed obviously Cotton effects at 575 nm, and no Cotton effects was found in the **BODIPY-βCD**-GSH, which indicated that the signal was only generated after the cross-coupling reaction between **BODIPY** and GS•. Compare to **BODIPY**-2GS•, the **BODIPY-βCD**-2GS• displayed more obvious Cotton effects, demonstrating that the presence of β-CD could induce the **BODIPY-βCD**-2GS• to produce a distinct circular dichroic signal. Meanwhile, as the concentration of GS• increased, the Cotton effects became more obvious (Figure S14a). In addition, we filled the **BODIPY-βCD** cavity with adamantane sodium formate (ADA-Na) to confirm the influence of cavity of β-CD (Figure S14b). As we expected, the Cotton effects of **BODIPY-βCD**-2GS• at 575 nm was declined, which indicated that the **BODIPY** unit was repalced by ADA-Na because of the strong host-guest interaction between adamantane and β-CD, confirming the **BODIPY** unit was encapsulated in the hydrophobic cavity. In order to confirm the assembly mode of **BODIPY-βCD**, we tested the 2D ROESY spectrum of **BODIPY-βCD** (1 mM) in D_2O. As shown in Figure S15, it can be seen that the signal of the **BODIPY** unit is obviously correlated with βCD, which confirms that the **BODIPY** unit is encapsulated in the βCD cavity. Subsequently, we compared the ^{1}H-NMR of **BODIPY-βCD** at 1 mM and 2 mM concentrations (Figure S16). The results show that as the concentration increases, the chemical shift of H in the **BODIPY** unit moves to the high field, demonstrating the assembly mode of **BODIPY-βCD** is intermolecular assembly. Therefore, we deduced that the **BODIPY** unit was wrapped inside the cavity of another molecule of β-CD after the **BODIPY-βCD**-2GS• was formed. The driving force may come from the hydrophobic interactions and hydrogen bond interactions between GSH and CD,[61] which was conducive to the formation of **BODIPY-βCD**-GS• assembly. In addition, the fluorescence quantum yields were measured to be 1.41% and 4.69% for **BODIPY** and **BODIPY-βCD**, as well as 33.45 % for **BODIPY**+2GS• and 56.43% for **BODIPY-βCD**+2GS•, respectively (Figure S17). This result displayed that the fluorescence quantum yields of **BODIPY** was significantly improved after covalent connecting with β-CD, which was suitable for bioimaging.

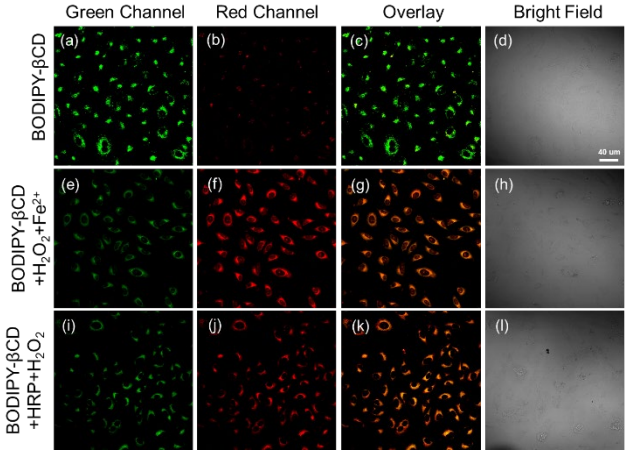

Figure 3 Confocal fluorescence images of living A549 cells incubated with (a–d) **BODIPY-βCD** (10 μM). (e–h) images of **BODIPY-βCD**-loaded A549 cells incubated with H_2O_2 and Fe^{2+} for additional 3 h. (i–l) images of **BODIPY-βCD**-loaded A549 cells incubated with HRP and H_2O_2 for additional 3 h. (Scale bar is 40 μm)

To explore the utility of the **BODIPY-βCD** for sensing of GS• in living cells, we first evaluated the cytotoxicity of **BODIPY-βCD** by means of CCK-8 assays. In comparison to a control group, the percentages (%) of cell viability displayed only a negligible change after incubation with different concentration of **BODIPY-βCD** for 24 h (Figure S18). This result demonstrated that **BODIPY-βCD** had an extremely low cytotoxicity. Subsequently, imaging of variations in cellular GS• was implement by using live A549 cells. As shown in Figure 3a–d, strong green fluorescence and weak red fluorescence were observed when the cells were incubated with **BODIPY-βCD** for 6 h. The result indicated that the **BODIPY-βCD** could be taken up by cells and gave a clear fluorescence signal. After that, when the cells were further treated with H_2O_2/Fe^{2+}, obvious enhance of red fluorescence was found, accompanied by the decline of fluorescence in the green channel (Figure 3e–h). This result revealed that the **BODIPY-βCD** could react with GS• and gave an obvious fluorescence signal change, confirming the excellent recognition ability of **BODIPY-βCD** for GS• in living cells. For the negative control experiments, we selected the NEM (N-Ethylmaleimide) as the scavenger of GSH, which could inhibit the generation of GS•. The cell was first treated with **BODIPY-βCD** for 6 h, and then added the NEM (0.5 mM) for another 1 h. Subsequently, the Fe^{2+} and H_2O_2 were added for additional 1.5 h, respectively. As shown in Figure S19a-d, upon addition of NEM, we can observe the strong green fluorescence and very weak red fluorescence. Moreover, the further processing of Fe^{2+} and H_2O_2 resulted in no significant increase in the red fluorescence channel (Figure S19e-h). The result demonstrated that the change in the fluorescence was caused by the fluxes of GS•. On the other hand, we also tested the HRP/H_2O_2/GSH systems in cell imaging. As shown in Figure 3i-l, when the cells were treated with HRP and H_2O_2, obvious enhance of red fluorescence was also found, accompanied by the decline of fluorescence in the green channel. This result revealed that the generation of GS• catalyzed by HRP and H_2O_2 in the presence of GSH, confirming the excellent recognition ability of BODIPY-βCD for GS• in living cells. To our knowledge, ferroptosis is an iron-dependent programmed cell death method.[62]Therefore, we anticipated that the **BODIPY-βCD** will provide a good method in the detection of GS•-related pathophysiological events during the process of ferroptosis.

Conclusions

In summary, we have constructed a unique ratiometric fluorescent probe based on **BODIPY** and β-CD through click reaction for high-sensitivity sensing of intracellular GS•. The **BODIPY-βCD** exhibited high affinity for GS• with the limits of detection for 468 nM, and the whole reaction can be finished within 10 min, accompanied by the observed rate constant (K_{obs}=3.18x10^{-3} s^{-1}) and a fast response time ($t_{1/2}$ = 218 s). A direct comparison between **BODIPY** and **BODIPY-βCD** was analyzed. Due to the existence of β-CD, the water solubility and biocompatibility were greatly increased, and the self-aggregation of **BODIPY** could be avoided, as well as the affinity and the sensitivity of **BODIPY-βCD** toward GS• was improved. In addition, not only limited to the Fenton reaction mediated by Fe^{2+}, the existence of HRP also can generate the GS• in the presence of H_2O_2 and GSH, and the **BODIPY-βCD** both displayed excellent ratiometric fluorescent response toward GS• during these two processes. The circular dichroism spectra displayed that the **BODIPY-βCD**+2GS• had obvious Cotton effects, demonstrating the **BODIPY** unit was encapsulated into the cavity of β-CD after reacted with GS•, accompanied by significant increase in fluorescence quantum yield. Cell imaging experiment indicated that the **BODIPY-βCD** had extremely low cytotoxicity, and can be employed to monitor GS• in live A549 cells, accompanied by excellent ratiometric fluorescence signal. In the present investigation, we expect that cyclodextrin-modified fluorescent probe will help to further detect GS• in biological systems.

Experimental

Solution preparation. **BODIPY-βCD** and **BODIPY** stock solution were made by dissolving them in DMSO. All above stock solution was prepared to a final concentration of 1 mM. GSH and other analyses were dissolved in water. In addition, all testing solutions were prepared by diluting stock solution with water. Mixing was usually done by adding analyte solution (for example, GSH, Fe^{2+} and H_2O_2 solution) into probe solution. HRP (150 unit/mg) was purchased from MACKLIN and the solution was made by dissolving it in water, and then reached the final concentration of 3 mg/mL. Cell staining solution was made by diluting 1 mM of **BODIPY-βCD** in water for a final probe concentration of 10 μM. The water were adjusted to different pH by using 1M NaOH solution and 1M HCl. The UV-Vis absorption changes and fluorescent spectra of **BODIPY-βCD** (10 μM) in water in the pH range of 4-10 were recorded with or without GS• (GSH+Fe^{2+}+H_2O_2).

Cell culture and fluorescence imaging experiment. A549 cells were grown in DMEM medium containing 10% FBS, 1% penicillin, and 1% streptomycin at 37 °C in 5% CO_2. Cells were plated on confocal dish and allowed to adhere for 24 hours. For confocal fluorescence imaging experiment, cells were incubated with **BODIPY-βCD** (10 μM) in culture medium for 6 h. After that, the Fe^{2+} (300 μM) or HRP (600 unit/mg) was added for 1.5 h, and then the H_2O_2 (300 μM) was added for another 1.5 h. In addition, for the negative experiments, the NEM (0.5 mM) was added for 1 h after treatment of **BODIPY-βCD**. Subsequently, the Fe^{2+} and H_2O_2 were added in the same way before cell imaging experiments. All the cell staining experiments were investigated after washing with PBS for 3 times. The excitation wavelengths for the green and red channels were 488 nm and 559 nm, and the emission wavelength ranges for the green and red channels were 500–550 and 575–650 nm, respectively.

Scheme 2 Synthesis of **BODIPY-βCD**.

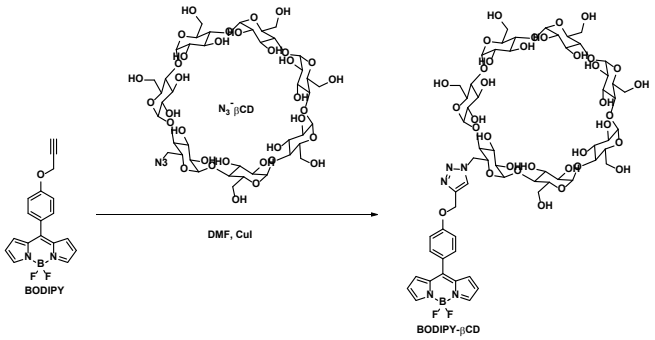

Synthesis of **N_3-βCD** and **BODIPY**: **N_3-βCD** and **BODIPY** were synthesized according to the reported procedure, respectively.[53,63]

Synthesis of **BODIPY-βCD**: **BODIPY** (50 mg, 0.16 mmol), **N_3-βCD** (172 mg, 0.16 mmol) and CuI (30 mg, 0.16 mmol) were dissolved in anhydrous DMF and the solution was stirred at 80℃ overnight. After that, the resultant residue was purified by silica gel chromatography to afford **BODIPY-βCD** (142.2 mg, 60%) as a orange solid.

^{1}H NMR (400 MHz, DMSO) δ 8.26 (s, 1H), 8.11 (s, 2H), 7.68 (d, *J* = 7.7 Hz, 2H), 7.29 (d, *J* = 8.0 Hz, 2H), 7.09 (s, 2H), 6.70 (s, 2H), 5.74 (m, 16H), 4.83 (m, 7H), 4.71 – 4.34 (m, 8H), 3.61 (m, 25H).

^{13}C NMR (100 MHz, DMSO) δ 160.84, 146.88, 143.84, 132.56, 131.53, 125.55, 118.93, 114.89, 101.90, 81.40, 72.90, 72.22, 71.94, 59.77, 30.57, 26.24.

HRMS-ESI (m/z): $[M+Na]^+$ calcd for $C_{60}H_{82}BF_2N_5O_{35}$: 1504.4749; found: 1504.4770.

Supporting Information

The supporting information for this article is available on the WWW under https://doi.org/10.1002/cjoc.2021xxxxx.

Acknowledgement (optional)

This work was supported by National Natural Science Foundation of China (grant numbers 21807038, 21772099, 21861132001) and by the China Postdoctoral Science Foundation (grant number 2019M651006).

References

(1) Trujillo, M.; Alvarez, B.; Radi, R. One- and two-electron oxidation of thiols: mechanisms, kinetics and biological fates. *Free. Radic. Res.* **2016,** *50*, 150.

(2) Sneeden, E. Y.; Hackett, M. J.; Cotelesage, J. J. H.; Prince, R. C.; Barney, M.; Goto, K.; Block, E.; Pickering, I. J.; George, G. N. Photochemically Generated Thiyl Free Radicals Observed by X-ray Absorption Spectroscopy. *J. Am. Chem. Soc.* **2017,** *139*, 11519.

(3) Schoneich, C. Thiyl radicals and induction of protein degradation. *Free. Radic. Res.* **2016,** *50*, 143.

(4) Moldéus, P.; O'Brien, P. J.; Thor, H.; Berggren, M.; Orrenius, S. Oxidation of glutathione by free radical intermediates formed during peroxidase-catalysed N-demethylation reactions. *FEBS Lett.* **1983,** *162*, 411.

(5) Zhao, R.; Lind, J.; Merenyi, G.; Eriksen, T. E. Kinetics of One-Electron Oxidation of Thiols and Hydrogen Abstraction by Thiyl Radicals from .alpha.-Amino C-H Bonds. *J. Am. Chem. Soc.* **1994,** *116*, 12010.

(6) Osburn, S.; Berden, G.; Oomens, J.; Gulyuz, K.; Polfer, N. C.; O'Hair, R. A. J.; Ryzhov, V. Structure and Reactivity of the Glutathione Radical Cation: Radical Rearrangement from the Cysteine Sulfur to the Glutamic Acid alpha-Carbon Atom. *ChemPlusChem* **2013,** *78*, 970.

(7) Winterbourn, C. C. Are free radicals involved in thiol-based redox signaling? *Free Radic. Biol. Med.* **2015,** *80*, 164.

(8) Lesslie, M.; Lau, J. K.-C.; Pacheco, G.; Lawler, J. T.; Michael Siu, K. W.; Hopkinson, A. C.; Ryzhov, V. Hydrogen atom transfer in metal ion complexes of the glutathione thiyl radical. *Int. J. Mass Spectrom.* **2018,** *429*, 39.

(9) Schöneich, C.; Dillinger, U.; von Bruchhausen, F.; Asmus, K.-D. Oxidation of polyunsaturated fatty acids and lipids through thiyl and sulfonyl radicals: Reaction kinetics, and influence of oxygen and structure of thiyl radicals. *Arch. Biochem. Biophys.* **1992,** *292*, 456.

(10) Borisenko, G. G.; Martin, I.; Zhao, Q.; Amoscato, A. A.; Kagan, V. E. Nitroxides scavenge myeloperoxidase-catalyzed thiyl radicals in model systems and in cells. *J. Am. Chem. Soc.* **2004,** *126*, 9221.

(11) Liu, Z.; Zhou, X.; Miao, Y.; Hu, Y.; Kwon, N.; Wu, X.; Yoon, J. A Reversible Fluorescent Probe for Real-Time Quantitative Monitoring of Cellular Glutathione. *Angew. Chem. Int. Ed.* **2017,** *56*, 5812.

(12) Umezawa, K.; Yoshida, M.; Kamiya, M.; Yamasoba, T.; Urano, Y. Rational design of reversible fluorescent probes for live-cell imaging and quantification of fast glutathione dynamics. *Nat. Chem.* **2017,** *9*, 279.

(13) Butler, J.; Hoey, B. M. Reactions of glutathione and glutathione radicals with benzoquinones. *Free Radic. Biol. Med.* **1992,** *12*, 337.

(14) Ramakrishna Rao, D. N.; Fischer, V.; Mason, R. P. Glutathione and ascorbate reduction of the acetaminophen radical formed by peroxidase. Detection of the glutathione disulfide radical anion and the ascorbyl radical. *J. Biol. Chem.* **1990,** *265*, 844.

(15) Stoyanovsky, D. A.; Maeda, A.; Atkins, J. L.; Kagan, V. E. Assessments of thiyl radicals in biosystems: difficulties and new applications. *Anal. Chem.* **2011,** *83*, 6432.

(16) Lee, S.; Li, J.; Zhou, X.; Yin, J.; Yoon, J. Recent progress on the development of glutathione (GSH) selective fluorescent and colorimetric probes. *Coordin. Chem. Rev.* **2018,** *366*, 29.

(17) Liu, Z.; Sun, X.; Dai, X.; Li, J.; Li, P.; Liu, Y. Sulfonatocalix[4]arene-based light-harvesting amphiphilic supramolecular assemblies for sensing sulfites in cells. *J. Mater. Chem. C* **2021,** *9*, 1958.

(18) Liu, Z.; Guo, S.; Piao, J.; Zhou, X.; Wu, X. A reversible fluorescent probe for circulatory detection of sulfites through a redox-based tandem reaction. *RSC Adv.* **2014,** *4*, 54554.

(19) Wang, L.; Hiblot, J.; Popp, C.; Xue, L.; Johnsson, K. Environmentally Sensitive Color-Shifting Fluorophores for Bioimaging. *Angew. Chem. Int. Ed.* **2020,** *59*, 21880.

(20) Wang, L.; Tran, M.; D'Este, E.; Roberti, J.; Koch, B.; Xue, L.; Johnsson, K. A general strategy to develop cell permeable and fluorogenic probes for multicolour nanoscopy. *Nat. Chem.* **2020,** *12*, 165.

(21) Tang, L.; Xia, J.; Zhong, K.; Tang, Y.; Gao, X.; Li, J. A simple AIE-active fluorogen for relay recognition of Cu2+ and pyrophosphate through aggregation-switching strategy. *Dyes Pigm.* **2020,** *178*, 108379.

(22) Bruemmer, K. J.; Crossley, S. W. M.; Chang, C. J. Activity-Based Sensing: A Synthetic Methods Approach for Selective Molecular Imaging and Beyond. *Angew. Chem. Int. Ed.* **2020,** *59*, 13734.

(23) Xiang, H.; Zhao, L.; Yu, L.; Chen, H.; Wei, C.; Chen, Y.; Zhao, Y. Self-assembled organic nanomedicine enables ultrastable photo-to-heat converting theranostics in the second near-infrared biowindow. *Nat. Commun.* **2021,** *12*, 218.

(24) Tian, M.; Liu, Y.; Jiang, F. L. On the Route to Quantitative Detection and Real-Time Monitoring of Glutathione in Living Cells by Reversible Fluorescent Probes. *Anal. Chem.* **2020,** *92*, 14285.

(25) Niu, L. Y.; Guan, Y. S.; Chen, Y. Z.; Wu, L. Z.; Tung, C. H.; Yang, Q. Z. BODIPY-based ratiometric fluorescent sensor for highly selective detection of glutathione over cysteine and homocysteine. *J. Am. Chem. Soc.* **2012,** *134*, 18928.

(26) Jung, H. S.; Chen, X.; Kim, J. S.; Yoon, J. Recent progress in luminescent and colorimetric chemosensors for detection of thiols. *Chem. Soc. Rev.* **2013,** *42*, 6019.

(27) Guo, Y.; Zheng, X.; Cao, X.; Li, W.; Wu, D.; Zhang, S. Reduced Thiol Compounds – Induced Biosensing, Bioimaging Analysis and Targeted Delivery. *Chin. J. Chem.* **2020,** *38*, 1793.

(28) Sheng, X.; Chen, D.; Cao, M.; Zhang, Y.; Han, X.; Chen, X.; Liu, S.; Chen, H.; Yin, J. A Near Infrared Cyanine-Based Fluorescent Probe for Highly Selectively Detecting Glutathione in Living Cells. *Chin. J. Chem.* **2016,** *34*, 594.

(29) Xiang, H. J.; Tham, H. P.; Nguyen, M. D.; Fiona Phua, S. Z.; Lim, W. Q.; Liu, J. G.; Zhao, Y. An aza-BODIPY based near-infrared fluorescent probe for sensitive discrimination of cysteine/homocysteine and glutathione in living cells. *Chem. Commun.* **2017,** *53*, 5220.

(30) Denes, F.; Pichowicz, M.; Povie, G.; Renaud, P. Thiyl radicals in organic synthesis. *Chem. Rev.* **2014,** *114*, 2587.

(31) Studer, A.; Curran, D. P. Catalysis of Radical Reactions: A Radical Chemistry Perspective. *Angew. Chem.Int. Ed.* **2016,** *55*, 58.

(32) Liu, C.; Liu, D.; Lei, A. Recent advances of transition-metal catalyzed radical oxidative cross-couplings. *Acc. Chem. Res.* **2014,** *47*, 3459.

(33) Ahangarpour, M.; Kavianinia, I.; Harris, P. W. R.; Brimble, M. A. Photo-induced radical thiol-ene chemistry: a versatile toolbox for peptide-based drug design. *Chem. Soc. Rev.* **2021,** *50*, 898.

(34) Ma, F.; Zhou, L.; Liu, Q.; Li, C.; Xie, Y. Selective Photocatalysis Approach for Introducing ArS Units into BODIPYs through Thiyl Radicals. *Org. Lett.* **2019,** *21*, 733.

(35) Lv, F.; Tang, B.; Hao, E.; Liu, Q.; Wang, H.; Jiao, L. Transition-metal-free regioselective cross-coupling of BODIPYs with thiols. *Chem. Commun.* **2019,** *55*, 1639.

(36) Lv, F.; Guo, X.; Wu, H.; Li, H.; Tang, B.; Yu, C.; Hao, E.; Jiao, L. Direct sulfonylation of BODIPY dyes with sodium sulfinates through oxidative radical hydrogen substitution at the alpha-position. *Chem. Commun.* **2020,** *56*, 15577.

(37) Treibs, A.; Kreuzer, F.-H. Difluorboryl-Komplexe von Di- und Tripyrrylmethenen. *Liebigs Ann. Chem.* **1968,** *718*, 208.

(38) Loudet, A.; Burgess, K. BODIPY dyes and their derivatives: syntheses and spectroscopic properties. *Chem. Rev.* **2007,** *107*, 4891.

(39) Boens, N.; Leen, V.; Dehaen, W. Fluorescent indicators based on BODIPY. *Chem. Soc. Rev.* **2012,** *41*, 1130.

(40) Kowada, T.; Maeda, H.; Kikuchi, K. BODIPY-based probes for the fluorescence imaging of biomolecules in living cells. *Chem. Soc. Rev.* **2015,** *44*, 4953.

(41) Liu, Z.; Dai, X.; Sun, Y.; Liu, Y. Organic supramolecular aggregates based on water‐soluble cyclodextrins and calixarenes. *Aggregate* **2020,** *1*, 31.

(42) Chen, G.; Jiang, M. Cyclodextrin-based inclusion complexation bridging supramolecular chemistry and macromolecular self-assembly. *Chem. Soc. Rev.* **2011,** *40*, 2254.

(43) Ji, X.; Ahmed, M.; Long, L.; Khashab, N. M.; Huang, F.; Sessler, J. L. Adhesive supramolecular polymeric materials constructed from macrocycle-based host-guest interactions. *Chem. Soc. Rev.* **2019,** *48*, 2682.

(44) Zhang, Y. M.; Liu, Y. H.; Liu, Y. Cyclodextrin-Based Multistimuli-Responsive Supramolecular Assemblies and Their Biological Functions. *Adv. Mater.* **2020,** *32*, e1806158.

(45) Mako, T. L.; Racicot, J. M.; Levine, M. Supramolecular Luminescent Sensors. *Chem. Rev.* **2019,** *119*, 322.

(46) Ma, X.; Zhao, Y. Biomedical Applications of Supramolecular Systems Based on Host-Guest Interactions. *Chem. Rev.* **2015,** *115*, 7794.

(47) Liu, Y.; You, C.-C. Molecular Recognition Studies on Modified Cyclodextrins. *Chin. J. Chem.* **2001,** *19*, 533.

(48) Sun, M.; Zhang, H.; Hu, X.; Liu, B.; Liu, Y. Hyperbranched Supramolecular Polymer of Tris(permethyl-β-cyclodextrin)s with Porphyrins: Characterization and Magnetic Resonance Imaging. *Chin. J. Chem.* **2014,** *32*, 771.

(49) Pan, T.; Zou, H.; Sun, H.; Liu, Y.; Liu, S.; Luo, Q.; Dong, Z.; Xu, J.; Liu, J. Construction of Redox Responsive Vesicles Based on a Supra-Amphiphile for Enzyme Confinement. *Chin. J. Chem.* **2017,** *35*, 871.

(50) Kanchana, U. S.; Diana, E. J.; Mathew, T. V.; Anilkumar, G. Cyclodextrin based palladium catalysts for Suzuki reaction: An overview. *Carbohydr. Res.* **2020,** *489*, 107954.

(51) Takahashi, K. Organic Reactions Mediated by Cyclodextrins. *Chem. Rev.* **1998,** *98*, 2013.

(52) Krishnaveni, N. S.; Surendra, K.; Rao, K. R. Study of the Michael addition

of beta-cyclodextrin-thiol complexes to conjugated alkenes in water. *Chem. Commun.* **2005**, 669.
(53) Liu, Z.; Zhou, W.; Li, J.; Zhang, H.; Dai, X.; Liu, Y.; Liu, Y. High-efficiency dynamic sensing of biothiols in cancer cells with a fluorescent β-cyclodextrin supramolecular assembly. *Chem. Sci.* **2020,** *11*, 4791.
(54) Li, J.; Cao, F.; Yin, H. L.; Huang, Z. J.; Lin, Z. T.; Mao, N.; Sun, B.; Wang, G. Ferroptosis: past, present and future. *Cell Death Dis.* **2020,** *11*, 88.
(55) Doll, S.; Conrad, M. Iron and ferroptosis: A still ill-defined liaison. *IUBMB Life* **2017,** *69*, 423.
(56) Chen, X. X.; Niu, L. Y.; Shao, N.; Yang, Q. Z. BODIPY-Based Fluorescent Probe for Dual-Channel Detection of Nitric Oxide and Glutathione: Visualization of Cross-Talk in Living Cells. *Anal. Chem.* **2019,** *91*, 4301.
(57) Wang, F.; Guo, Z.; Li, X.; Li, X.; Zhao, C. Development of a small molecule probe capable of discriminating cysteine, homocysteine, and glutathione with three distinct turn-on fluorescent outputs. *Chem. Eur. J.* **2014,** *20*, 11471.
(58) Liu, X. L.; Niu, L. Y.; Chen, Y. Z.; Zheng, M. L.; Yang, Y.; Yang, Q. Z. A mitochondria-targeting fluorescent probe for the selective detection of glutathione in living cells. *Org. Biomol. Chem.* **2017,** *15*, 1072.
(59) Gong, D.; Han, S. C.; Iqbal, A.; Qian, J.; Cao, T.; Liu, W.; Liu, W.; Qin, W.; Guo, H. Fast and Selective Two-Stage Ratiometric Fluorescent Probes for Imaging of Glutathione in Living Cells. *Anal. Chem.* **2017,** *89*, 13112.
(60) Liu, X. L.; Niu, L. Y.; Chen, Y. Z.; Yang, Y.; Yang, Q. Z. A multi-emissive fluorescent probe for the discrimination of glutathione and cysteine. *Biosens. Bioelectron.* **2017,** *90*, 403.
(61) Garcia-Fuentes, M.; Trapani, A.; Alonso, M. J. Protection of the peptide glutathione by complex formation with alpha-cyclodextrin: NMR spectroscopic analysis and stability study. *Eur. J. Pharm. Biopharm.* **2006,** *64*, 146.
(62) Aron, A. T.; Loehr, M. O.; Bogena, J.; Chang, C. J. An Endoperoxide Reactivity-Based FRET Probe for Ratiometric Fluorescence Imaging of Labile Iron Pools in Living Cells. *J. Am. Chem. Soc.* **2016,** *138*, 14338.
(63) Lou, X. Y.; Song, N.; Yang, Y. W. Enhanced Solution and Solid-State Emission and Tunable White-Light Emission Harvested by Supramolecular Approaches. *Chem. Eur.J.* **2019,** *25*, 11975.

(The following will be filled in by the editorial staff)
Manuscript received: XXXX, 2021
Manuscript revised: XXXX, 2021
Manuscript accepted: XXXX, 2021
Accepted manuscript online: XXXX, 2021
Version of record online: XXXX, 2021

Entry for the Table of Contents

Fluorescence Sensing of Glutathione Thiyl Radical by BODIPY-Modified β-Cyclodextrin

Zhixue Liu, Xianyin Dai, Qiaoyan Xu, Xiaohan Sun, and Yu Liu*

Chin. J. Chem. **2021**, *39*, XXX—XXX. **DOI: 10.1002/cjoc.202100XXX**

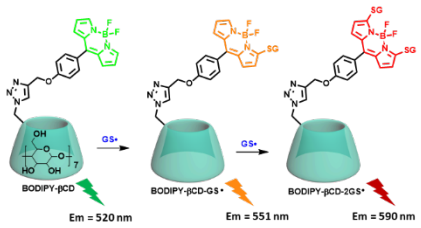

A unique ratiometric fluorescent probe was developed by BODIPY-modified β-cyclodextrin based on cross-coupling reaction between thiol radicals and BODIPY. The probe not only shows good water solubility and biocompatibility, but also enables high-sensitive detecting of glutathione thiyl radical in cancer cells.

[a] *Department, Institution, Address 1*
E-mail:

[b] *Department, Institution, Address 2*
E-mail:

[c] *Department, Institution, Address 3*
E-mail: